Sensitivity of Train Path Envelopes for Automatic Train Operation

Wang, Ziyulong; Quaglietta, Egidio; Bartholomeus, Maarten; Goverde, Rob M.P.

DOI
10.1109/TITS.2025.3590628

Publication date
2025

Document Version
Final published version

Published in
IEEE Transactions on Intelligent Transportation Systems

Sensitivity of Train Path Envelopes for Automatic Train Operation

Ziyulong Wang, Egidio Quaglietta, Maarten Bartholomeus, and Rob M. P. Goverde, *Member, IEEE*

***Abstract*— Automatic Train Operation (ATO) aims to enhance punctuality, energy efficiency, and reliability by automating driving tasks. Specifically, for mainline railways, an ATO onboard component generates and tracks optimised train trajectories based on time targets or windows at critical network locations, known as timing points, across train routes. These timing points and their associated constraints are specified in the Train Path Envelope (TPE), computed to ensure conflict-free operations. The generation of TPEs relies on dynamic updates of the real-time traffic plan from the Traffic Management System and real-time train statuses (e.g., position and speed). Understanding how TPEs are affected by these updates is essential for effective ATO deployment. To address this, this paper proposes a sensitivity analysis using elementary effects of a TPE generation algorithm, evaluating its response to variations in real-time traffic plans and train status updates. A real-life case study on a Dutch rail corridor with heterogeneous traffic reveals that control timing points can be introduced into the TPE as headways decrease, to homogenise traffic by aligning speed profiles and thus resolving conflicts. Timing point locations remain mostly unchanged, while their associated time windows become more sensitive when placed further along the route. Operational tolerance, which defines the latest conflict-free passing time, becomes more sensitive to headway changes and the distance from the previous stop.**

***Index Terms*— Automatic train operation, traffic management system, train path envelope, sensitivity analysis.**

I. Introduction

AUTOMATIC Train Operation (ATO) aims at assisting or automating train driving tasks to improve running time reliability, energy efficiency and punctuality. While ATO is widely implemented in urban and metro railways with predefined train trajectories or coasting strategies [1], this study focuses on ATO in mainline railways. In this context, the ATO onboard component generates and tracks optimised train trajectories, adhering to arrival, departure, or passing times at specific locations known as Timing Points (TPs) [2], [3]. Previous work has proposed to use critical network locations as TPs to determine their time windows, which constitute a Train Path Envelope (TPE) that serves as constraints for generating each train's conflict-free trajectory [4], [5]. In this paper, conflict-free operation refers to the absence of blocking time overlaps between successive trains, ensuring that movement authorities can be extended without triggering braking or restrictive signalling [6].

The TPE is aligned with the Real-Time Traffic Plan (RTTP) from the Traffic Management System (TMS), which specifies train routes with reference locations and times and may incorporate rescheduling decisions such as retiming, reordering, and rerouting [7], [8]. The TMS dynamically maintains a conflict-free RTTP through proactive conflict detection and resolution, which is then translated into train-level trajectory constraints through the TPE computation, while the RTTP is also used for route setting and informing all other actors to guarantee an aligned coordination between train operations and traffic control. Real-time train statuses are also utilised to compute an effective TPE, ensuring its adaptability to evolving conditions.

Dynamic changes in RTTP updates and train status reports can affect the TPE, introducing fluctuations to the train trajectory generation constraints used by ATO onboard algorithms. Such variability may lead to infeasible trajectories or uncomfortable changes in train driving regimes, particularly when planning assumptions no longer hold. However, the sensitivity of TPEs to variations in RTTP updates and train statuses has not been studied yet in the literature.

To address this gap, this paper performs a sensitivity analysis using elementary effects [9] of the TPE computation under varying operational inputs at the short-term operational planning level, as part of the Europe's Rail FP1-MOTIONAL project [5]. These inputs include RTTP variations, represented by planned headway adjustments, and train status changes, reflected through speed and position updates. The analysis quantifies the importance of these inputs and the extent to which their variations influence the computed TPs and their associated time targets or timing windows along the train route. This form of sensitivity analysis supports early-stage evaluation of operational robustness prior to closed-loop microscopic simulation or integration testing [10], and helps guide the alignment between discrete-event-based traffic management and continuous-speed-based train control. The contributions of this paper are threefold:

- Proposing a sensitivity analysis using elementary effects to quantify the impact of planned headways from the

Received 10 January 2025; revised 28 May 2025; accepted 11 July 2025. This work was supported Europe's Rail Joint Undertaking under the European Union's Horizon 2022 Research and Innovation Programme under Grant 101101973 (FP1-MOTIONAL). The Associate Editor for this article was M. Sallak. *(Corresponding author: Ziyulong Wang.)*

Ziyulong Wang, Egidio Quaglietta, and Rob M. P. Goverde are with the Department of Transport and Planning, Delft University of Technology, 2600 GA Delft, The Netherlands (e-mail: z.wang-19@tudelft.nl; e.quaglietta@tudelft.nl; r.m.p.goverde@tudelft.nl).

Maarten Bartholomeus is with the Department of ERTMS Central Systems, ProRail, 3511 EP Utrecht, The Netherlands (e-mail: maarten.bartholomeus@prorail.nl).

Digital Object Identifier 10.1109/TITS.2025.3590628

RTTP and updates in train statuses on the locations and time windows of timing points from the TPE generation;
- Applying the proposed method to a real-life case study on a Dutch rail corridor with heterogeneous traffic, demonstrating the effects of headway and status variability on TPE feasibility and responsiveness;
- Identifying when the TPE can effectively resolve conflicts via speed adjustment alone, and when replanning from the TMS is needed to maintain conflict-free operations.

The remainder of this paper is structured as follows: we provide a literature review in Section II followed by the methodology in Section III. Then, we present and discuss the results in Section IV. Finally, Section V concludes the paper.

II. Literature Review

A. Automatic Train Operation

ATO can partially or totally automate train driving functions. Five Grades of Automation (GoA) for ATO are defined in [11], ranging from manual on-sight driving (GoA 0) to fully unattended driving (GoA 4). From ATO GoA 2 onwards, train traction and braking commands are automated between successive stops for improvements in schedule adherence, capacity, energy efficiency and cost effectiveness compared to manual driving behaviour [1]. While ATO has been widely adopted in metro systems, its implementation remains largely conceptual for mainline railways with linking to a TMS. This is primarily due to the complexities, such as heterogeneous rail traffic and complex operating environments [4].

To facilitate the implementation of ATO in mainline railways, recent advancements have led to technical specifications of ERTMS/ATO within the European Rail Traffic Management System (ERTMS) [2], [3]. Figure 1 illustrates the ERTMS/ATO reference architecture. Within this architecture, the European Train Control System (ETCS) onboard, operating as a safety-critical component, continuously supervises the ATO onboard using a dynamic speed profile until the end of the movement authority. The ATO trackside generates a Journey Profile, which comprises a list of Segment Profiles (representing route data), along with TP constraints and temporary restrictions (e.g., additional speed limitations and adhesion conditions) [3]. This Journey Profile incorporates the TPE, thereby guiding the ATO onboard in generating conflict-free train trajectories while adhering to the current timetable. Furthermore, the ATO onboard provides the train status reports back to the ATO trackside, concerning the position, speed, and estimated arrival time at the upcoming TPs of a train [2].

The current specifications do not standardise the interaction between the TMS and ATO, particularly regarding the role of the ATO trackside. It is not specified which component computes the conflict-free TPEs. The TPEs may either be provided by the TMS, with the ATO trackside taking a passive role in transmitting them to the ATO onboard or actively generated by the ATO trackside itself before being sent to the ATO onboard. Besides, the feedback loops from ATO onboard status reports are also not standardised: the ATO trackside may either forward these reports to the TMS for traffic optimisation or use them to re-optimise the TPEs in a direct loop between the ATO onboard and trackside, enabling faster control responses. Determining the effective interaction between RTTP updates and TPE generation, including the necessary feedback mechanisms, is currently under investigation as part of [5].

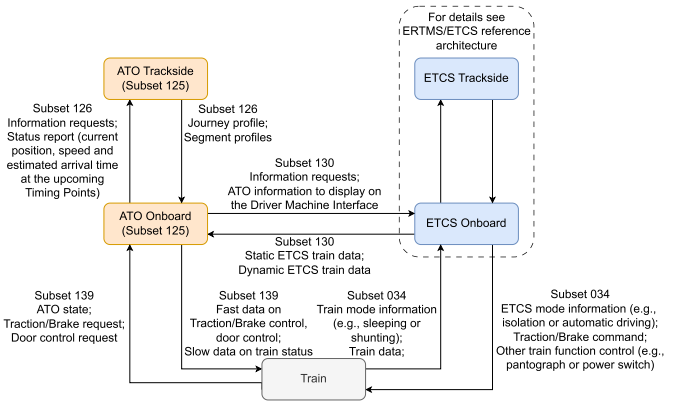

Fig. 1. ERTMS/ATO reference architecture, adapted from [2].

B. Related Work to Train Path Envelope

Considerable literature exists on the development of TMS functions aimed at dynamically computing up-to-date schedules or RTTPs [7], [12], [13], [14]. Despite this, automated railway traffic conflict detection and resolution are not yet applied in practice. Consequently, only a few attempts have been made to link TMS and train operation effectively.

On the one hand, traffic management can be integrated with train operation. For example, an integrated approach presented in [15] computes conflict-free train trajectories at the TMS to derive train trajectory targets for the ATO. Similarly, some approaches utilise approximate discrete train speed profiles as a decision variable to jointly compute dispatching and train control solutions for minimising train delays [16] or energy consumption [17]. This integration strategy is also developed in metro operations, where the objective typically revolves around optimising the energy efficiency of both the timetable and train operation [18], [19]. Additionally, research has explored the selection of a suitable speed profile from a pre-generated set to achieve the same objective [20], [21].

On the other hand, the concept of a TPE is introduced to provide constraints in the form of time targets or windows at TPs for the train trajectory generation problem [7], [22]. This TPE defines an envelope around possible train trajectories, facilitating energy-efficient train operation while meeting timetable punctuality requirements [23], [24]. However, TPEs computed for all trains using the given RTTP may not always ensure conflict-free operations. Therefore, a timetable constraint set has been proposed to fine-tune the values of time targets or windows at stations [25], which was further developed to achieve conflict-free energy-efficient timetables [26]. Moreover, adding control TPs between stops can enforce sufficient separation between trains by imposing time windows that trains must adhere to at these points [27], [28], [29]. To compute conflict-free TPEs for various trains,

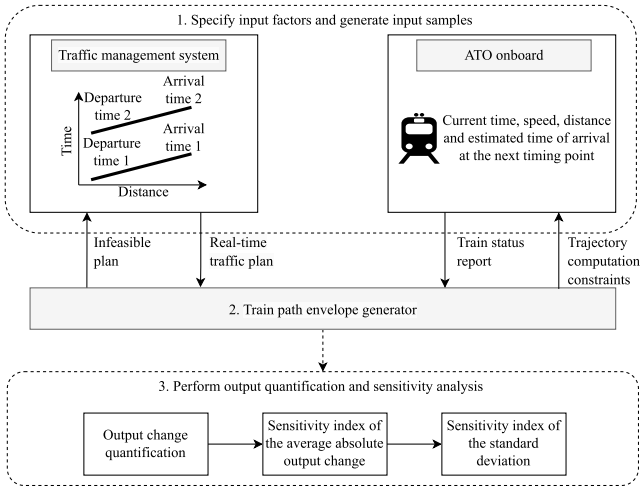

Fig. 2. Overview of the TPE sensitivity analysis in response to RTTP updates and train status changes.

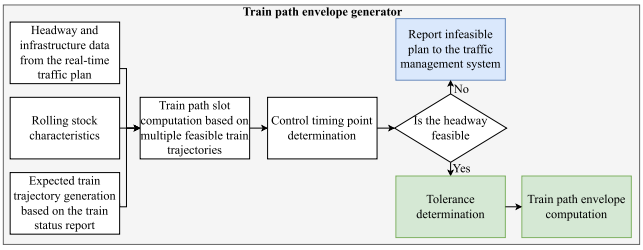

Fig. 3. Overview of the TPE generator.

Wang et al. [30] developed a method to optimise the locations of TPs and their associated time windows, facilitating effective ATO onboard train trajectory generation and execution.

The sensitivity of the TPE with respect to regular updates of the RTTP and the stochastic evolution of rail traffic conditions over time has not been investigated yet. Understanding this sensitivity is crucial for identifying critical thresholds in variations of planned headways within the RTTP, as well as in train speeds and positions, to avoid infeasible trajectory generation or uncomfortable driving regime changes executed by the ATO onboard. This issue is closely tied to practical challenges in the development of ATO technologies.

III. Methodology

Based on the identified research gap, this paper investigates the sensitivity of TPEs in relation to variations in headways derived from rescheduled event times in the RTTP at the TMS, as well as dynamic changes in train speeds and positions based on feedback from train status reports provided by ATO onboards. An overview of the methodology is presented in Figure 2 and elaborated in the subsequent subsections. Section III-A introduces the overall problem of TPE generation sensitivity. Section III-B explains the TPE concept and the key computational steps implemented in the TPE generator, as illustrated in Figure 3. These steps include input data extraction, step-wise bandwidth blocking time computation (termed Train Path Slot, TPS) from multiple feasible trajectories, overlapping blocking time detection and resolution by determining control TPs and tolerances, and TPE construction to constrain ATO onboard trajectory generation. If conflicts cannot be resolved, infeasibility is reported to the TMS. Sections III-C and III-D describe the influence of RTTP updates and train status reports, respectively. Finally, Section III-E presents the sensitivity analysis using elementary effects to evaluate output variations.

A. Problem Description and Assumptions

This study investigates the sensitivity of TPE computation to variations in two key input sources, namely planned train headways from the RTTP and dynamic train status updates, including train positions and speeds. The analysis focuses on how these variations affect the outputs of the TPE generation, i.e., the computed departure tolerances at scheduled stops, the time windows at control TPs, and the operational tolerances during train operations. Quantifying these sensitivities provides insights into the feasibility and flexibility of the generated TPEs under different operational conditions.

The TPE computation aligns discrete-event-based RTTP updates from the TMS with continuous-speed-based trajectory generation at the ATO onboard system. Specifically, the TMS maintains a conflict-free RTTP through proactive conflict detection and resolution, and the TPE computation translates this plan into trajectory constraints for the ATO onboard system at the short-term operational planning level [7]. The TPE defines a bounded range of feasible train trajectories that ensure punctual arrival at the next stop, determined by the earliest and latest trajectories under different driving strategies.

To construct the TPE, we generate multiple feasible train trajectories under different driving strategies and derive their corresponding blocking times. The blocking time represents the exclusive track use, which comprises a setup time, sight and reaction time, the approach time to the block section, the running time within the block, the clearing time during which the train vacates the block over its entire length, and the release time of the route [31]. The subsequent blocking times of a train form a blocking time stairway in a time-distance diagram, while the compression of these stairways for successive trains determines the infrastructure occupation over a corridor [31]. This paper focuses on radio-based fixed-block signalling systems, such as ETCS Level 2 with trackside train detection [32], but the proposed method can also be applied to traditional fixed-block multi-aspect signalling or moving block systems, which all fit the generic blocking time theory.

A conflict occurs when a train reaches its braking curve indication point, meaning it is too close to a block section still occupied by a preceding train and therefore must begin braking [6]. Such conflicts are detected through overlapping blocking times, which reflect both interlocking rules and signalling constraints (e.g., ETCS). For train operations to remain conflict-free, the blocking times of successive trains must not overlap within the same block section. This separation allows the following train to receive timely movement authority extensions and proceed without unnecessary braking. Potential blocking time conflicts are resolved by enforcing the earliest passage times at control TPs for the following train and adjusting the departure tolerance of the preceding train,

thereby regulating train speed profiles. These adjustments result in a discrete set of TPs with associated time constraints, which together define the TPE and guide conflict-free train trajectory generation. If the TPE computation cannot resolve the conflict, the TMS is notified and must compute an updated RTTP to provide a revised conflict-free plan, e.g., due to insufficient line headway. Recall from Figure 1 that ETCS provides safety-critical speed and distance supervision. The corresponding constraints on train separation are modelled in the blocking times.

We assume a static computational setting, where the RTTP and train status reports are available instantaneously. The TPE is computed once per input configuration, representing an updated RTTP and train states. This enables a focused sensitivity analysis on key inputs: line headway, train position, and train speed. Communication between the ATO onboard and the ATO trackside occurs via Train-to-Ground, while communication between the TMS and ATO trackside occurs via Ground-to-Ground. No direct Train-to-Train communication is involved.

B. Train Path Slot and Train Path Envelope

The TPE generator in Figure 3 implements the computational steps by considering multiple train driving strategies to compute the step-wise bandwidth blocking times (i.e., TPS) and resolving potential blocking time conflicts. This subsection explains the underlying concepts of TPS and TPE computation, control TP determination, and tolerance adjustment, which together enable the construction of a conflict-free TPE.

Typically, TMS algorithms assume a deterministic train trajectory to (re)schedule the timetable and provide an RTTP. This RTTP normally contains only target departure/arrival/passing event times at stations or junctions, which are adequate to ensure conflict-free train operations. The (re)scheduling process often involves presuming a Reduced Maximum Speed (RMS) train driving strategy, where trains cruise at a constant speed below the track speed limit to meet the target arrival time [33]. However, a train can follow various trajectories while satisfying the dynamic equations of motion and complying with the same target arrival time at its next stop. One such trajectory is based on the Energy-Efficient Train Control (EETC), incorporating both cruising and coasting regimes [34], [35]. Overlap(s) in blocking time between EETC- and RMS-based train paths can occur, requiring additional control TPs beyond the reference locations and times provided by the RTTP to resolve the conflicts. A particularly efficient method to mitigate these overlaps involves optimising TPs at critical blocks associated with the train trajectories [30]. Specifically, critical block(s) are identified using the timetable compression method and indicate the block with either the shortest time between consecutive blocking times or the largest overlap in case of conflicts [31].

Let $p \in P$ denote a train, and $(p_i, p_j) \in P_2$ represent an ordered successive pair of trains, where p_i precedes p_j. A control TP for train p_j, denoted as $s \in S_{p_j}$, is assigned at the entry location s_b of a shared critical block section $b \in B_{p_i} \cap B_{p_j}$. This critical block is defined by the largest blocking time overlap, $c^{\max}_{p_i,p_j}$, between these two trains. The passing time of train p_j at this control TP determines the earliest passage time at this critical block to avoid a conflict. In response to the added control TP, a TP Response (TPR) driving strategy adapts the train speed profile by combining RMS and EETC profiles. It employs a lower cruising speed to meet the added control TP and uses the remaining running time supplement for coasting during the later stages, thereby avoiding conflicts with other trains (see [30] for more details).

Furthermore, train departures may experience slight delays within an acceptable tolerance as long as a feasible trajectory exists for the train to reach its destination by the scheduled arrival time. This tolerance, derived from the allocated running time supplement, absorbs minor deviations from the planned schedule by establishing an upper bound on the train trajectories and enhances the robustness of train paths, provided there are no blocking time overlaps. The tolerance reaches its maximum when the train departs late up to the scheduled running time supplement and adopts the Minimum-Time Train Control (MTTC) strategy operating as fast as possible [35], [36], which is termed Shifted MTTC (SMTTC). To determine the tolerance of the preceding train p_i, it is initially set to the running time supplement and fine-tuned until either there are no blocking time overlaps or it reduces to zero. The Departure Tolerance Response (DTR) driving strategy is assumed as an RMS driving strategy that departs at the updated tolerance and arrives on time at the next stopping point.

Wang et al. [30] introduced the TPS as a step-wise bandwidth that includes the blocking time stairways of selected train driving strategies, such as RMS, EETC, and, where feasible, SMTTC, allowing the train to arrive on time at its destination. The TPS spans between the start of the blocking time of the earliest train trajectory (until that block) and the end of the blocking time of the latest train trajectory. We offer an example with three successive RMS-based blocking time stairways as in the TMS (re)scheduling algorithms, alongside the three corresponding initial TPSs integrating RMS and EETC strategies, as shown in Figure 4 (a) and (b). This example unfolds along an approximately 50-km-long railway corridor with varying gradients and speed limits. This illustration highlights the TPS overlap between the first and second trains (from bottom to top), requiring tolerance adjustments and possibly adding a control TP for the second train.

Figure 4 (c) presents the final three successive TPSs with optimised sets of TPs. It shows that the first train's tolerance is zero, the second is reduced from 195 (full running time supplement) to 141 seconds, and the third remains full. A control TP with a time window is defined at 30.285 km for the second train, and the associated time window is calculated based on the block entry time difference between different driving strategies. Lastly, the TPs are assembled in a TPE to be forwarded to the ATO onboard, which adds flexibility to the ATO onboard train trajectory generation.

C. Train Path Envelopes and TMS Updates

Daily railway operations may deviate from the schedule due to unforeseen events, e.g., extended running or dwell

TABLE I
DIFFERENT LINE HEADWAYS AND THEIR ASSUMED DRIVING STRATEGIES

Line Headway Type	Meaning	Preceding Train Strategy	Following Train Strategy
TPS headway	Minimum robust line headway allowing all assumed driving strategies	All	All
Nominal driving headway	Minimum conflict-free line headway considering multiple driving strategies that comply with scheduled departure and arrival times, with zero tolerance for the preceding train at departure	RMS & EETC	RMS & EETC
Minimum line headway with one single driving strategy	Minimum conflict-free line headway using the same driving strategy of both trains	RMS | EETC | MTTC	RMS | EETC | MTTC
TPR headway	Minimum line headway with controlled following train, assuming no changes to scheduled departure and arrival events, with the following train reaching the control TP at its earliest permissible time and the preceding train following punctual driving strategies	RMS & EETC	TPR

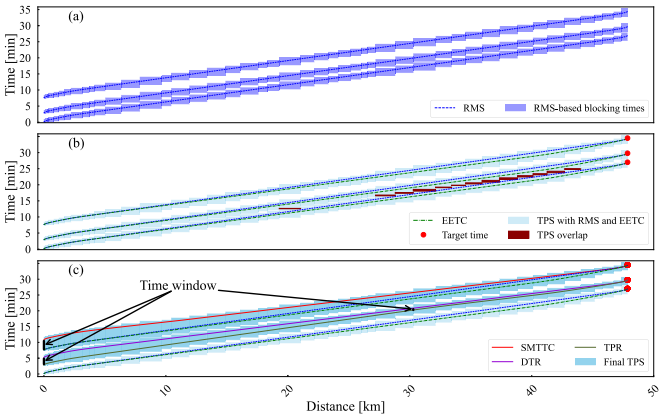

Fig. 4. (a) Example of three successive conflict-free RMS-based blocking time stairways. (b) Example of three successive initial TPSs with only one target time and TPS overlaps, integrating RMS and EETC driving strategies. (c) Example of the three successive final TPSs with optimised sets of TPs.

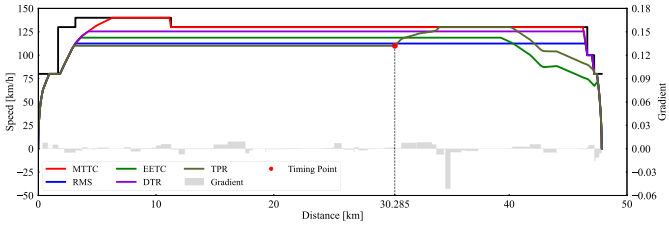

Fig. 5. Example speed profiles of selected train driving strategies.

times. These traffic disturbances are monitored and predicted by the TMS, namely relatively small path deviations without modifying the resources. If conflicts are detected, the TMS resolves them and offers an updated RTTP. Various control measures pertaining to retiming, reordering and rerouting, impact the RTTP by altering scheduled event times, which also implies adjusting train separation distances and times. These altered event times will influence the TPE determination.

In this subsection, line headways corresponding to various (re)scheduled event times within the RTTP serve as critical inputs for determining conflict-free train operations. A line headway is defined as the minimum time interval between successive train departures at the first station of a corridor that ensures conflict-free operations over their routes. These line headways represent potential RTTP variations for successive train paths, categorised into four boundary types, as summarised in Table I and detailed below.

Let $t_{p,b}^{E,\gamma}$ and $t_{p,b}^{L,\gamma}$ denote the running times to block b for train p according to the earliest and latest train trajectories, which depend on a specific driving strategy γ, where $\gamma \in \Gamma = \{\text{RMS, EETC, TPR, SMTTC, DTR, TPS}\}$. In particular, the TPS driving strategy is a special case representing a bundle of selected driving strategies. Figure 5 illustrates the various speed profiles corresponding to the time-distance diagrams presented in Figure 4 under identical conditions. The train trajectory modelling is specific to each train, accounting for speed limits, gradients, and train-dependent parameters.

The corresponding start of the blocking time for a train p at a given block section $b \in B_p$ over a designated railway corridor with multiple stops is represented by:

$$\underline{t}_{p,b}^{E,\gamma} = t_{p,b}^{E,\gamma} - t_{p,b}^{E,\text{approach},\gamma} - t_{p,b}^{E,\text{reaction}} - t_{p,b}^{E,\text{setup}} - t_{p}^{E,\text{buffer}}, \tag{1}$$

where $t_{p,b}^{E,\text{approach},\gamma}$ denotes the approach time of train p to block b for the driving strategy γ, $t_{p,b}^{E,\text{reaction}}$ is a constant parameter representing the ATO reaction time, and $t_{p,b}^{E,\text{setup}}$ signifies the setup time within block b, depending on whether the block is on open tracks or in interlocking areas. Fixed buffer times, denoted as $t_{p}^{E,\text{buffer}}$ at the start and $t_{p}^{L,\text{buffer}}$ at the end of the blocking time, may be included to mitigate delay propagation for timetable robustness and provide tolerance for train trajectory tracking algorithms.

The corresponding end of the blocking time is given by:

$$\bar{t}_{p,b}^{L,\gamma} = t_{p,b}^{L,\gamma} + t_{p,b}^{L,\text{run},\gamma} + t_{p,b}^{L,\text{clear},\gamma} + t_{p,b}^{L,\text{release}} + t_{p}^{L,\text{buffer}}, \tag{2}$$

where $t_{p,b}^{L,\text{run},\gamma}$ represents the running time of train p in block b, and $t_{p,b}^{L,\text{clear},\gamma}$ denotes the time for train p to clear the block

b based on a specific driving strategy γ. Additionally, $t^{L,\text{release}}_{p,b}$ is a constant parameter used to release block b.

The minimum line headway between trains p_i and p_j over this corridor for the given train trajectories is given by the maximum overlap when the successive train paths are scheduled to depart simultaneously:

$$h^{\gamma_i,\gamma_j}_{p_i,p_j} = \max_{b \in B_{p_i} \cap B_{p_j}} \left(\bar{t}^{L,\gamma_i}_{p_i,b} - \underline{t}^{E,\gamma_j}_{p_j,b} \right). \tag{3}$$

This minimum line headway time is the minimum time separation between two train paths at the line start, ensuring conflict-free train operations. The critical block for this train pair p_i, p_j where the successive blocking times are closest is the block $b^*_{p_i,p_j}$ where the maximum is achieved:

$$b^*_{p_i,p_j} = \operatorname*{argmax}_{b \in B_{p_i} \cap B_{p_j}} \left(\bar{t}^{L,\gamma_i}_{p_i,b} - \underline{t}^{E,\gamma_j}_{p_j,b} \right). \tag{4}$$

The critical block does not have to be unique when multiple blocks are at the same shortest time distance. In the compressed timetable, all blocks other than the critical block(s) have positive buffer time between the successive trains.

The minimum robust line headway $h^{\text{TPS}}_{p_i,p_j}$ that allows all assumed driving strategies is termed a TPS headway. In eqs. (1) to (4), this corresponds to $\gamma_i = \gamma_j = \text{TPS}$, where TPS includes the RMS, EETC and SMTTC driving strategies. As the line headway decreases, the robustness of the train path declines due to reduced tolerance. When this tolerance is no longer feasible, a second nominal driving headway $h^{\text{Nom}}_{p_i,p_j}$ is determined. This nominal driving headway is defined as the minimum departure interval required for conflict-free operations when a successive train pair may use various driving strategies with punctual departure and arrival. In this case, the SMTTC driving strategy is excluded from the calculations of the previous instance. Third, the minimum line headway for the same driving strategy of both trains $h^{\gamma}_{p_i,p_j}$ is defined as the interval when a train pair operates under a specific driving strategy without DTR or TPR. This headway is computed from eqs. (1) to (4) with $\gamma_i = \gamma_j \in \{\text{RMS, EETC, MTTC}\}$. For completeness, we include the MTTC driving strategy here as it corresponds to a theoretical minimum line headway based on an assumed deterministic train trajectory.

The three line headway types mentioned earlier are applicable in undisturbed conditions. However, the TPE can include extra control TPs with time windows for potentially conflicting train pairs to avoid conflicts caused by a faster-following train trajectory. This situation can arise when the following train applies the EETC driving strategy and accelerates to a higher cruising speed to optimise coasting phases at later stages. In this case, the preceding train adheres to nominal driving strategies with $\gamma_i = \text{TPS}$, while the following train follows the TPR strategy $\gamma_j = \text{TPR}$ in eqs. (1) to (4). Without altering the scheduled departure and arrival times of a train pair, the minimum TPR headway $h^{\text{TPS, TPR}}_{p_i,p_j}$ is computed by determining the latest permissible passage time of the following train at the critical block to ensure conflict-free operations. If the actual headway is shorter than the TPR headway, indicating that the interval between trains is insufficient to resolve the conflict, then the TMS must provide an updated RTTP. In this case, the TPE computation cannot determine a feasible set of train trajectory generation constraints.

D. Train Path Envelopes and Train Status Updates

During operations, the ATO onboard sends train status reports, which are used to optimise or adjust the TPE or the RTTP if the TPE cannot be respected. These reports include the current time t, location $x_{p,t}$, speed $v_{p,t}$, and estimated time of arrival at the next TP, t_{p,σ_p}, where $\sigma_p = \sigma_p(x_{p,t})$ returns the next TP with a time target after the current location $x_{p,t}$. This information is represented as a measurement vector $\hat{a}_{p,t}$:

$$\hat{a}_{p,t} = \left[t, x_{p,t}, v_{p,t}, t_{p,\sigma_p} \right]^T. \tag{5}$$

Given the known initial and terminal states of the train, including its start and end times and locations, train trajectories can be computed for both before and after the current position, namely the realised and expected trajectories. The realised train trajectory leads to realised blocking times up to (but excluding) the current block section $b(x_{p,t})$, denoted by superscript r, as $[\underline{t}^{E,r}_{p,b'}, \bar{t}^{L,r}_{p,b'}]$ for blocks $b' \in B^r_p(x_{p,t})$, where $B^r_p(x_{p,t}) = \left\{ b' \in B_p \mid s_{b'} \in [0, b(x_{p,t})) \right\}$. Here, $b(x)$ is defined as a function that maps a position x to the corresponding block section containing that position. The expected TPS represents the range of blocking times for blocks in the upcoming route of the train, represented by $[\underline{t}^{E,\text{TPS}}_{p,b}, \bar{t}^{L,\text{TPS}}_{p,b}]$ for blocks $b \in B^e_p(x_{p,t})$, where $B^e_p(x_{p,t}) = \left\{ b \in B_p \mid s_b \in (b(x_{p,t}), b(\sigma_p(x_{p,t}))) \right\}$. This expected TPS is derived using RMS, EETC, and operational tolerance response driving strategies (described below), reflecting the possible behaviour of the train in the future based on its current position and speed. Upon receiving a measurement within a specific block section, we define the realised blocking time start as the lower contour and the expected TPS end as the upper contour of the current block section, i.e., $[\underline{t}^{E,r}_{p,b(x_{p,t})}, \bar{t}^{L,\text{TPS}}_{p,b(x_{p,t})}]$. This representation captures the infrastructure occupation status, combining the actual movement of the train to its current position with the expected range of blocking times ahead.

To compute the operational tolerance response driving strategy, we assume that the train applies maximum traction promptly upon sending the latest measurement, if applicable, and operates at the maximum feasible speed for the remainder of the journey. As a result of this driving strategy, the train would arrive early, denoted as t'_{p,σ_p}, compared to the originally estimated time of arrival t_{p,σ_p}. The difference between these two arrival times constitutes the operational tolerance, denoted as $d_{p,t} = t_{p,\sigma_p} - t'_{p,\sigma_p}$. This tolerance is used to shift the response driving strategy upon sending the latest measurement such that the scheduled arrival time can be met. The operational tolerance defines the latest permissible passing time at the moment the preceding train status report is received without inducing blocking time conflicts. It constrains the feasible train trajectories from that point onward and serves as an upper bound for ATO onboard trajectory

generation, supporting cruising speed regulation and coasting adjustments.

Information on realised blocking times and expected TPSs within a railway traffic corridor is denoted as $\widetilde{\mathrm{TPS}}_p(t)$ and used for the dynamic generation and adjustment of the TPE. Due to potential asynchronicity in transmitting status reports from each train, previously expected TPSs remain valid until updated. The information $\widetilde{\mathrm{TPS}}_p(t)$ is hence given by:

$$\begin{aligned}\widetilde{\mathrm{TPS}}_p(t) = \Big\{ &\Big\{ \Big[\underline{t}^{E,r}_{p,b'},\, \bar{t}^{L,r}_{p,b'} \Big],\ b' \in B^r_p(x_{p,t}) \Big\}, \\ &\Big\{ \Big[\underline{t}^{E,r}_{p,b(x_{p,t})},\, \bar{t}^{L,\mathrm{TPS}}_{p,b(x_{p,t})} \Big] \Big\}, \\ &\Big\{ \Big[\underline{t}^{E,\mathrm{TPS}}_{p,b},\, \bar{t}^{L,\mathrm{TPS}}_{p,b} \Big],\ b \in B^e_p(x_{p,t}) \Big\} \Big\}. \end{aligned} \tag{6}$$

The TPE generation algorithm is re-executed upon receiving a new train status report or at regular intervals, to identify additional required control TPs, fine-tune tolerances or adjust previously determined TPE to enhance train operations. Any newly added control TPs are positioned downstream after the current block. The associated critical blocks must be assessed to determine if sufficient distance is available to incorporate them and enable the TPR driving strategy. Initially determined TPEs with fine-tuned tolerances or control TPs can be relaxed or adjusted if no or less TPS overlap is detected. This adjustment can improve flexibility in train operations and enhance energy efficiency. For example, cruising at a higher speed and extending coasting can be achieved by expanding or removing the time window constraint at a control TP.

E. Sensitivity Analysis Using Elementary Effects

Tightly (re)scheduled times within the RTTP may not always yield a feasible TPS headway, while variability in train behaviour, as reflected in status reports from the ATO onboard, impacts the flexibility needed to adopt driving strategies that meet the objectives of the railway undertakings, such as passenger comfort and energy efficiency. The dynamic evolution of rescheduling measures at the TMS, combined with realised and expected train trajectories and corresponding track occupations, highlights the need to evaluate their effects on generating conflict-free TPEs.

Our sensitivity analysis uses an approach based on the concept of elementary effects, which capture those changes in an output solely due to changes in a particular input, as introduced in [9]. This method evaluates the sensitivity of the model output to variations in individual input factors by systematically isolating and varying them over their entire feasible range. This approach requires no assumptions on input sparsity, output monotonicity, or smooth functional approximations, making it suitable for the multi-stage, optimisation-based TPE generator.

Consider a function $f(\mathbf{x})$ with n input factors, represented as a vector $\mathbf{x} = (x_1, x_2, \ldots, x_n)$. The elementary effect E_i of an input factor x_i is calculated by changing x_i with a defined step Δ_i while holding other factors fixed. The method evaluates $n_i + 1$ evenly spaced sample points within the specified range $[\underline{x}_i, \bar{x}_i]$, where the step size is given by $\Delta_i = (\bar{x}_i - \underline{x}_i)/n_i$. These sample points $x_{i,j}$ are generated along the trajectory as $x_{i,j} = \underline{x}_i + (j-1)\cdot\Delta_i$, where $j = 1, 2, \ldots, n_i$, representing the positions of x_i at which its sensitivity is evaluated. The first elementary effect $E_{i,1}$ represents the initial change at $j = 1$, while the general j-th elementary effect $E_{i,j}$ describes the sensitivity at any subsequent j in the parameter space of x_i. The elementary effect $E_{i,j}$ at each point $x_{i,j}$ is calculated as:

$$E_{i,j} = \frac{f(x_1, \ldots, x_{i-1}, x_{i,j} + \Delta_i, x_{i+1}, \ldots, x_n) - f(x_1, \ldots, x_{i-1}, x_{i,j}, x_{i+1}, \ldots, x_n)}{\Delta_i}, \tag{7}$$

which represents the gradient of function f at $x_{i,j}$ over the interval defined by the step Δ_i. Since each elementary effect requires two adjacent points, the maximum number of elementary effects for each parameter is constrained to n_i. By evaluating each sample point $x_{i,j}$ along a trajectory, we can obtain a distribution of elementary effects, capturing the variability in the sensitivity of f to changes in x_i. For each input factor x_i, we calculate the mean effect μ_i, and the standard deviation σ_i, which serve as sensitivity indices to quantify the influence of changes in elementary effects E_i:

$$\mu_i = \frac{1}{n_i} \sum_{j=1}^{n_i} E_{i,j}, \tag{8}$$

$$\sigma_i = \sqrt{\frac{1}{n_i - 1} \sum_{j=1}^{n_i} \left(E_{i,j} - \mu_i\right)^2}. \tag{9}$$

These indices capture the average impact and variability of the influence of each factor on the model output, respectively. A higher mean effect μ_i indicates that an input consistently and strongly influences the output. In contrast, a higher standard deviation σ_i implies that the effect of the input varies across the input space, often due to nonlinearities or interactions. These indices jointly characterise the importance and behaviour of each input with respect to the model output. Algorithm 1 summarises the computational steps involved in performing the sensitivity analysis using elementary effects.

We begin by analysing the input space of the TPE computation and identifying the most influential factors, i.e., line headway, train position, and train speed. These inputs are then varied in a controlled manner to explore their impact through sensitivity analysis. In our sensitivity analysis, we focus on three TPE model output functions f, corresponding to departure tolerance, the placement of a control TP with its associated time window, and the operational tolerance as defined below. Since a control TP is only generated under sufficiently small headways, these functions are treated separately, each defined over a different headway range.

The first function $f_1(h)$ denotes the tolerance at departure, which depends only on the line headway h. When the headway between two trains is sufficiently large, $f_1(h)$ alone constitutes the TPE in the form of a departure tolerance. However, when $f_1(h)$ is zero, an additional time constraint at a control TP

Algorithm 1 Sensitivity Analysis Using Elementary Effects for TPE Computation

Input: A scalar-valued TPE model output $f(\mathbf{x})$;
Input factors $\mathbf{x} = (x_1, x_2, \ldots, x_n)$ with respective bounds $[\underline{x}_i, \bar{x}_i]$
Output: Sensitivity indices (mean effect μ_i, standard deviation σ_i) for each input factor x_i
for *each input factor* x_i **do**
  Generate $n_i + 1$ evenly spaced sample points $x_{i,j}$ in range $[\underline{x}_i, \bar{x}_i]$ with step size $\Delta_i = (\bar{x}_i - \underline{x}_i)/n_i$;
  for *each point* $x_{i,j}$ **do**
    Compute elementary effect $E_{i,j}$ using eq. (7);
  Compute mean sensitivity index μ_i using eq. (8);
  Compute standard deviation sensitivity index σ_i using eq. (9);
return μ_i, σ_i *for all* i

may become necessary. The second function $f_2(h)$ represents the time window at an introduced control TP, which also depends on the line headway h, and is defined over the range of headway values for which $f_1(h) = 0$, i.e., when the departure tolerance is determined to be zero and the blocking time conflict remains, requiring an additional constraint at a control TP. For both $f_1(h)$ and $f_2(h)$, the input factor h is bounded by the minimum and the maximum headway values derived from the RTTP for a specific train pair.

The range between the TPS headway and the nominal driving headway, and the range between the nominal driving headway and the TPR headway, define the feasible adjustment ranges for the departure tolerance of the preceding train and the time window at the control TP for the following train, respectively. The sensitivity indices provide insight into the responsiveness of the computed departure tolerance and time window to headway changes, particularly in relation to the spatial positioning of TPs. A low mean effect μ_h indicates that headway has limited overall influence on the TPE model outputs, while a low standard deviation σ_h suggests that this influence remains consistent across different headway values.

The third function $f_3(h, x, v)$ represents the operational tolerance during a train run and is a function of line headway h, position x and speed v. Given the interdependence of time, speed, and distance in trajectory generation, speed v is chosen as the input factor to quantify variations in operational tolerance, while h and x define the traffic scenario and the measurement location. Adjustments to speed v are applied within the permissible range set by the original TPE at the selected position x and headway h. These adjustments are constrained by the minimum and maximum speeds of the selected train trajectories within the original TPE.

The sensitivity indices for operational tolerance indicate how variations in speed, headway, or position affect the flexibility available during train operation. A high mean effect μ_v reflects a strong and consistent influence of speed across different positions and headways, while a high standard deviation σ_v suggests that this influence depends on the specific traffic scenario. The results inform where trains may require closer adherence to reference trajectories, or where greater driving flexibility is possible. They also support identifying locations requiring additional buffer times or upstream traffic measures. Although not direct TMS or ATO commands, these indices reflect the dynamic use of the running time supplement.

IV. Case Study and Results

A. Case Study Description

Our case study is conducted on a Dutch rail corridor, spanning 22 kilometres between Breda (Bd) and Tilburg (Tb) stations. This corridor includes intermediate stations Gilze-Rijen (Gz), Tilburg Reeshof (Tbr), and Tilburg Universiteit (Tbu). The maximum corridor speed limit is 140 km/h.

The case study assumes ETCS Level 2 with fixed blocks, which provides continuous supervision of speed and braking curves [32]. Key parameters are configured as follows: $t_{p,b}^{\text{release}} = 2$ s, $t_{p,b}^{\text{reaction}} = 1$ s, $t_{p,b}^{\text{setup}} = 1$ s (for open track segments), or $t_{p,b}^{\text{setup}} = 6 \times$ number of switches in seconds (in station areas or junctions), and $t_p^{E,\text{buffer}} = t_p^{L,\text{buffer}} = 10$ s (added to the TPS lower and upper contours for the original timetable but not in the following sensitivity analyses).

In a periodic schedule with half an hour cycle time between stations Bd and Tb, two freight (FR) trains and three passenger trains are modelled. Among these, there is one Sprinter (SPR) train (i.e., local train) that stops at every station, alongside two Intercity (IC) trains that only serve stations Bd and Tb. The FR trains pass station Bd at 0.5 min and 14 min, while the SPR train departs from station Bd to Tb at 23 min. Additionally, the two IC trains depart from station Bd at 8 and 20 min. The service braking rates of IC, SPR and FR trains are -0.8 m/s^2, -0.66 m/s^2, and -0.5 m/s^2 respectively.

The initial and optimised TPSs for the original timetable in the Breda-Tilburg corridor are depicted in Figure 6 (a) and (b). The TPS overlaps are identified between the IC departing at 20 min and the SPR departing at 23 min from station Bd, with a maximum overlap of 102 s, as highlighted by the red overlaps in Figure 6 (a). This overlap can be resolved by adjusting the tolerance of the preceding IC train at station Bd to 50 s without the need for additional control TPs, as shown in Figure 6 (b).

B. Train Path Envelope Sensitivity to TMS Updates

The first sensitivity analysis examines the relationship between the (re)planned line headways at station Bd from a potentially updated RTTP and the TPEs across all possible train pairs in the case study. All permutations of three representative train types are tested, independent of the original timetable sequence, covering distinct line headways for each pair. Headway values are computed as described in the methodology (Table II), and sensitivity is evaluated at departure stations and control TPs. The analysis spans the full headway range in 3 s intervals, and the resulting indices for tolerance and time window adjustments are presented

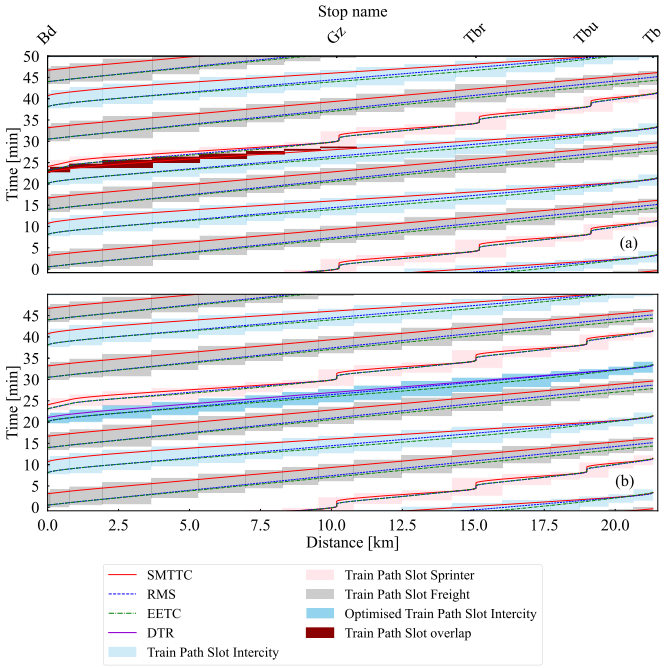

Fig. 6. (a) Initial (top) and (b) optimised TPSs (bottom) for the original timetable in the Breda-Tilburg corridor.

TABLE II

COMPUTED LINE HEADWAYS [S] FOR ALL POSSIBLE TRAIN PAIRS

Train Pair	$h^{\text{TPS}}_{p_i,p_j}$	$h^{\text{Nom}}_{p_i,p_j}$	$h^{\text{EETC}}_{p_i,p_j}$	$h^{\text{RMS}}_{p_i,p_j}$	$h^{\text{MTTC}}_{p_i,p_j}$	$h^{\text{TPS, TPR}}_{p_i,p_j}$
IC - IC	261	162	126	132	141	132
IC - FR	309	162	156	156	159	102
IC - SPR	264	117	111	117	114	87
FR - IC	303	237	189	192	243	189
FR - FR	282	153	141	144	138	141
FR - SPR	237	114	96	102	120	114
SPR - IC	447	432	420	432	423	432
SPR - FR	375	369	375	321	258	369
SPR - SPR	231	198	180	180	192	198

in Table III and Table IV. Cells marked with dashes (–) denote cases where control TPs are inapplicable due to critical blocks occurring at or near the next scheduled stop. For train pairs with two indices, multiple tolerances or time windows are computed, with further explanation provided below. Figure 7 visualises the relationship between headway and the departure tolerance for the preceding train (solid lines) and the time window at the control TP for the following train (dashed lines).

Considering heterogeneous train pairs, especially where a faster train follows a slower one, we observe that the resulting headway tends to be larger due to the running time differences between trains. This phenomenon is particularly notable when SPR trains precede in a train pair, owing to their extended time-distance train path with multiple intermediate stops. In such cases, the critical block of a train pair occurs at or close to the next scheduled stop, resulting in the TPR headway coinciding with the nominal headway. This is also seen in the FR-SPR train pair, where the critical block is located at station

TABLE III

SENSITIVITY ANALYSIS OF TOLERANCE AT ATO TIMING POINTS ON THE HEADWAY GRID FOR CASE STUDY TRAIN PAIRS

Train Pair	Departure Timing Point	Headway Range [s] Min	Max	Sensitivity Indices of Tolerance μ_h	σ_h
IC - IC	Bd	162	261	1.60	0.84
IC - FR	Bd	162	309	1.04	0.15
IC - SPR	Bd	117	264	1.03	0.16
FR - IC	Bd	237	303	2.16	0.56
FR - FR	Bd	153	282	1.11	0.20
FR - SPR	Bd	114	237	1.20	0.33
SPR - IC	Tbu	432	441	2.07	0.28
SPR - FR	Tbu	369	375	5.00	0.24
SPR - SPR	Tbr	198	231	0.94	0.14
	Tbu			1.08	0.14

TABLE IV

SENSITIVITY ANALYSIS OF TIME WINDOW AT ATO CONTROL TIMING POINTS ON THE HEADWAY GRID FOR CASE STUDY TRAIN PAIRS

Train Pair	Timing Point Location [m]	Headway Range [s] Min	Max	Sensitivity Indices of Time Window μ_h	σ_h
IC - IC	14,248	132	162	1.04	0.27
IC - FR	1,929	102	162	0.81	0.19
IC - SPR	1,929	87	117	0.64	0.20
FR - IC	16,027	189	237	1.06	0.28
FR - FR	6,817	141	153	1.17	0.11
	16,027			0.61	1.02
FR - SPR	-	114	114	-	-
SPR - IC	-	432	432	-	-
SPR - FR	-	369	369	-	-
SPR - SPR	-	198	198	-	-

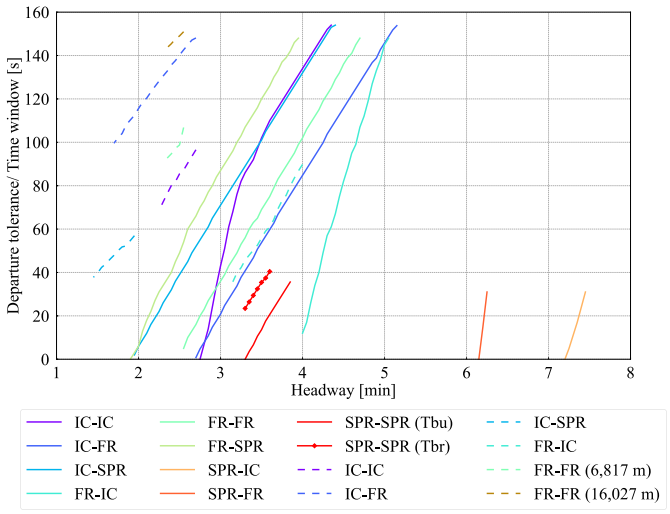

Fig. 7. Relationship between headway and tolerance for the preceding train (solid line) and headway and time window at the control timing point (dashed line) for the following train across all train pairs in the case study.

Gz. In these instances, it is not possible to utilise a control TP to resolve the train path conflicts.

Heterogeneous train pairs, where SPR or FR precedes, exhibit higher mean sensitivity indices (μ_h) for departure tolerance adjustments, indicating that headway has a consistently strong influence on train pairs where slower trains precede. In such cases, the impact on departure tolerance can be twice as large or more compared to the reverse sequence. This effect

is particularly pronounced when the conflicting block lies beyond the halfway point of the corridor from the previous stop. For SPR trains, shorter inter-stop distances and limited running time supplements further constrain tolerance adjustments. The passing pattern of FR trains also amplifies this effect, requiring larger adjustments to maintain a conflict-free upper contour in the TPS under the DTR strategy. The SPR-FR pair shows the highest mean effect ($\mu_h = 5.00$), reflecting a steep and consistent increase in departure tolerance adjustments as headway decreases, consistent with the pronounced slope in Figure 7 (second orange line from the right).

In contrast, train pairs with an IC preceding typically exhibit lower mean sensitivity indices (μ_h), as conflicts occur earlier in the corridor and the longer scheduled running times allow more flexibility to absorb headway variations through small tolerance changes. Low mean sensitivity indices (μ_h) are also observed for homogeneous train pairs. In particular, in the SPR-SPR pair, reducing the headway from 213 s to 210 s requires fine-tuning tolerances at both stations Tbr and Tbu.

The IC-IC pair, however, is a notable exception, exhibiting a distinct slope change midway through the headway range (around 3.2 min), as shown by the purple line in Figure 7. This shift corresponds to a rise in the standard deviation (σ_h), indicating that the influence of headway on the departure tolerance becomes more variable across the headway range. This behaviour arises from the DTR strategy, where reducing cruising speed prolongs running and clearing times while shortening the approach time compared to SMTTC. As a result, the blocking time overlap shifts beyond the midpoint of the corridor (12,471 m), requiring larger adjustments.

For the time window sensitivity at control TPs, heterogeneous train pairs, such as IC-SPR and IC-FR, exhibit lower mean sensitivity indices (μ_h) compared to homogeneous pairs. This is primarily because control TPs are introduced earlier along the corridor, allowing more flexibility in the form of running time supplements. For instance, the control TP is located at 1,929 m for the following SPR and FR trains in the IC-SPR and IC-FR pairs, respectively, whereas it appears much later at 14,248 m for the IC-IC pair. Time window sensitivity increases at later TPs due to longer travel distances and less remaining running time supplement. For example, the control TP at 16,027 m exhibits a higher μ_h than those placed earlier. Notably, when the headway is reduced from 153 s to 150 s for the FR-FR train pair, two control TPs are introduced simultaneously to maintain conflict-free operation. When an SPR train leads, the critical block often coincides with a scheduled stop, making it infeasible to define control TPs for resolving conflicts through speed adjustment.

Figure 7 highlights a sudden drop in the time window for the FR-FR train pair at 6,817 m (dashed turquoise line). This deviation occurs because the first control TP requires substantial adjustment from the original passing time computed using the EETC strategy. As the train already passes later at the first control TP, the time window adjustment at the second becomes comparatively smaller. However, the standard deviation of the sensitivity index at 16,027 m ($\sigma_h = 1.02$) is significantly higher than at 6,817 m ($\sigma_h = 0.11$), indicating that the effect of headway on the time window at the second TP is influenced by nonlinearities or interactions between the two control TPs and the degree of headway variation. Consequently, the difference between the original and adjusted time windows at the first and second control points is pronounced.

Overall, adjustments for departure tolerances and time windows show a decreasing trend as headway is reduced. The mean effect μ_h on time window is generally lower than on departure tolerance, reflecting the narrower adjustment range under the TPR strategy. This strategy maintains a steady cruising speed up to the control TP to avoid conflicts, while the remaining running time supplement is used for EETC driving. In contrast, the DTR strategy uses the running time supplement by lowering cruising speeds between stops, enabling broader tolerance adjustments with stronger influence.

C. Train Path Envelope Sensitivity to Train Status Updates

The second sensitivity analysis investigates a case study featuring the IC train departing at 20 min and the SPR train at 23 min in the original timetable, which showed TPS overlaps (recall Figure 6 (a)). The scheduled headway of 180 s is reduced to 150 s and 120 s to evaluate its impact on the TPEs of both trains. The analysis examines various cruising speeds of the IC train within the bounds of the original TPE, considering distances of 5 km, 10 km, and 15 km, based on its scheduled running time of 810 s between stations Bd and Tb. Train speed is incrementally increased by 5 km/h, ranging from 103.48 km/h (RMS) to 134.40 km/h (SMTTC) at 5 km, from 103.48 km/h (RMS) to 140 km/h (SMTTC) at 10 km, and from 101.20 km/h (EETC) to 140 km/h (SMTTC) at 15 km. The resulting sensitivity indices, presented in Table V, quantify the impact of speed changes on the operational tolerance of the IC train at each distance and headway.

The results show that when the headway is above the nominal driving headway between these two trains (in this case, 117 s) and the preceding train stays within the original TPE, there is no need to introduce control TPs for the following train. In general, the tolerance at specific points increases with higher cruising speeds to that point, as a greater portion of the running time supplement remains available for operational adjustments. This enables ATO onboard systems to adopt EETC with coasting while respecting the conflict-free operation constraints. Additionally, larger headways offer a larger buffer between trains, further increasing the robustness.

Nevertheless, TPS overlaps between trains impose a tolerance limit for conflict-free operations. For example, under a 150-second headway, the tolerance stabilises at 62.48 s for speeds from 115 km/h at 5 km and 120.58 s for speeds from 130 km/h at 10 km. Figure 8 illustrates that increasing speed beyond certain thresholds does not yield a higher tolerance due to TPS constraints, as shown by the impact of a status report speed of 120 km/h at 10 km under a 150-second headway.

In conflict-free scenarios, such as those at 15 km, operational tolerance remains consistent when the running time supplement is fully utilised, with the MTTC strategy starting at the computed tolerance and arriving at the next target time. By contrast, when conflicts are consistently present or absent

TABLE V
SENSITIVITY ANALYSIS OF ATO TIMING POINTS FOR THE IC-SPR TRAIN PAIR AT VARYING HEADWAYS AND DISTANCES

Speed [km/h]	**Operational Tolerance [s] at Various Distances and Headways**								
	5 km			**10 km**			**15 km**		
	120 s	**150 s**	**180 s**	**120 s**	**150 s**	**180 s**	**120 s**	**150 s**	**180 s**
105	22.43	53.86	83.33	40.76	70.85	80.07	40.78	40.78	40.78
110	24.50	57.51	88.15	53.39	84.20	94.89	63.08	63.08	63.08
115	24.50	62.48	92.87	64.22	95.73	107.54	82.97	82.97	82.97
120	24.50	62.48	96.15	64.22	106.05	119.00	100.47	100.47	100.47
125	24.50	62.48	97.14	64.22	114.46	128.09	115.58	115.58	115.58
130	24.50	62.48	97.14	64.22	120.58	136.28	128.64	128.64	128.64
135	-	-	-	64.22	120.58	141.03	137.73	137.73	137.73
140	-	-	-	64.22	120.58	145.60	145.60	145.60	145.60
Sensitivity index μ_v	0.07	0.29	0.46	0.59	1.24	1.64	2.62	2.62	2.62
Sensitivity index σ_v	0.17	0.45	0.45	1.09	1.11	0.98	1.45	1.45	1.45

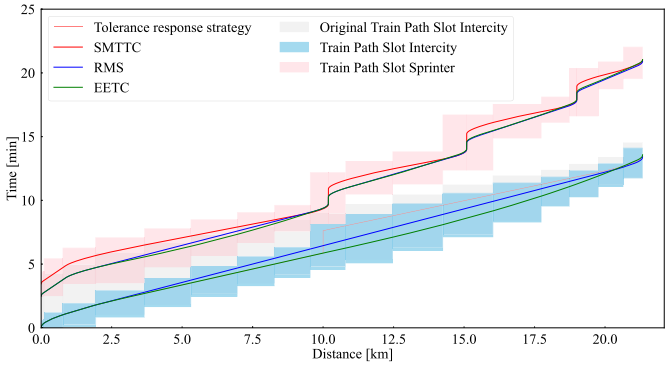

Fig. 8. Comparison of the original and operational TPSs for the preceding IC train, alongside the original TPS for the following SPR train, with a 150-second headway and a status report sent at 120 km/h at 10 km.

across headways and the running time supplement is not fully consumed, the difference in operational tolerance corresponds to the headway difference, for instance, at 5 km with a speed of 105 km/h. Slight variations in operational tolerance also arise from applying the tolerance response strategy as an RMS driving strategy, where arrival time deviations in the computation process lead to minor differences in the results.

The sensitivity indices reveal that operational tolerance is less affected by speed variations when the train is closer to its previous stop (e.g., at 5 km), where only a small portion of the running time has elapsed and speed deviations have limited opportunity to accumulate. This is reflected by low mean (μ_v) and standard deviation (σ_v), indicating limited influence and a consistent response. In such cases, operational tolerance is smaller, and maintaining a speed profile close to the reference trajectory is critical to remain within the TPE. At greater distances (e.g., 10 km and 15 km), speed deviations accumulate more significantly, increasing both μ_v and σ_v, and indicating stronger and more input-dependent effects. These findings confirm and extend the headway-based analysis, where operational tolerance becomes more sensitive at greater distances and responds more strongly to changes in headway and speed. Although greater tolerance allows for more flexibility in applying energy-efficient strategies such as coasting, it also reflects a higher responsiveness to input variation. In such situations, onboard speed regulation using the TPE may be insufficient, and an RTTP update from the TMS may be required to maintain conflict-free operation.

While the sensitivity indices provide insights into the responsiveness of TPE generation against input variations, their absolute values are mainly meaningful within the same TPE model output and infrastructure segment. The departure tolerance, the time window at control TPs, and the operational tolerance all represent time-based flexibility in relation to the allocated running time supplement along the train route but serve distinct operational purposes. Consequently, although the sensitivity analysis enables cross-line measurement for a specific model output, comparison across different model outputs requires contextual interpretation.

V. CONCLUSION

This study investigated the sensitivity of the Train Path Envelope (TPE) for Automatic Train Operation (ATO) to variations in real-time traffic plans and train status report updates. The TPE comprises time targets or windows at relevant locations along train routes, serving as constraints for conflict-free train trajectory generation by the ATO onboard. A sensitivity analysis using elementary effects was proposed to evaluate how variations in planned headways within the RTTP and reported train speeds and positions influence the computation of conflict-free TPEs.

The analysis showed that while the spatial structure of the TPE remains unchanged under reduced headways, the associated time windows become increasingly constrained, particularly for heterogeneous train pairs with differing running times and critical blocks positioned further along their routes. For train status updates, operational tolerance becomes more sensitive to speed variations as the train moves further from its previous stop, due to the accumulation of early speed deviations and a reduction in the available running time supplement. These findings support reducing infrastructure occupation by homogenising train trajectories through the addition of a control TP, which enables shorter line headways compared to the unrestricted case where departure tolerance is available. Low sensitivity indices indicate limited input influence and sufficient onboard driving flexibility through TPE adjustments. In contrast, high indices reflect larger and potentially nonlinear changes in TPE model outputs in response to input variations, which may necessitate RTTP updates.

Future research will focus on embedding the TPE generator within a closed-loop microscopic simulation environment to

evaluate the dynamic behaviour of TPEs and their interactions with the TMS and ATO under scenarios involving disturbances, disruptions, and human factors.

ACKNOWLEDGMENT

The authors would like to thank Dick Middelkoop and Vincent Weeda from ProRail for providing the necessary data for this study.

REFERENCES

[1] J. Yin, T. Tang, L. Yang, J. Xun, Y. Huang, and Z. Gao, "Research and development of automatic train operation for railway transportation systems: A survey," *Transp. Res. C, Emerg. Technol.*, vol. 85, pp. 548–572, Dec. 2017.

[2] *ERTMS/ATO—System Requirements Specification*, document SUBSET-125, UNISIG, 2023.

[3] *ERTMS/ATO–ATO-OB / ATO-TS FFFIS Application Layer*, document SUBSET-126, UNISIG, 2023.

[4] Z. Wang, E. Quaglietta, M. G. P. Bartholomeus, and R. M. P. Goverde, "Assessment of architectures for automatic train operation driving functions," *J. Rail Transp. Planning Manage.*, vol. 24, Dec. 2022, Art. no. 100352.

[5] *TMS and ATO/C-DAS Timetable Test & Simulation Environment*, Europe's Rail, Bern, Switzerland, 2024.

[6] R. M. P. Goverde, F. Corman, and A. D'Ariano, "Railway line capacity consumption of different railway signalling systems under scheduled and disturbed conditions," *J. Rail Transp. Planning Manage.*, vol. 3, no. 3, pp. 78–94, Aug. 2013.

[7] E. Quaglietta et al., "The ON-TIME real-time railway traffic management framework: A proof-of-concept using a scalable standardised data communication architecture," *Transp. Res. C, Emerg. Technol.*, vol. 63, pp. 23–50, Feb. 2016.

[8] S. Tschirner, B. Sandblad, and A. W. Andersson, "Solutions to the problem of inconsistent plans in railway traffic operation," *J. Rail Transp. Planning Manage.*, vol. 4, no. 4, pp. 87–97, Dec. 2014.

[9] M. D. Morris, "Factorial sampling plans for preliminary computational experiments," *Technometrics*, vol. 33, no. 2, pp. 161–174, May 1991.

[10] *Standard for Models and Simulations*, Standard NASA-STD-7009B, 2024.

[11] *Railway Applications–Urban Guided Transport Management and Command/control Systems—Part 1: System Principles and Fundamental Concepts*, IEC Standard 62290-1, 2014.

[12] V. Cacchiani et al., "An overview of recovery models and algorithms for real-time railway rescheduling," *Transp. Res. B, Methodol.*, vol. 63, pp. 15–37, May 2014.

[13] P. Pellegrini, G. Marlière, R. Pesenti, and J. Rodriguez, "RECIFE-MILP: An effective MILP-based heuristic for the real-time railway traffic management problem," *IEEE Trans. Intell. Transp. Syst.*, vol. 16, no. 5, pp. 2609–2619, Oct. 2015.

[14] W. Fang, S. Yang, and X. Yao, "A survey on problem models and solution approaches to rescheduling in railway networks," *IEEE Trans. Intell. Transp. Syst.*, vol. 16, no. 6, pp. 2997–3016, Dec. 2015.

[15] X. Rao, M. Montigel, and U. Weidmann, "A new rail optimisation model by integration of traffic management and train automation," *Transp. Res. C, Emerg. Technol.*, vol. 71, pp. 382–405, Oct. 2016.

[16] X. Luan, Y. Wang, B. De Schutter, L. Meng, G. Lodewijks, and F. Corman, "Integration of real-time traffic management and train control for rail networks—Part 1: Optimization problems and solution approaches," *Transp. Res. B, Methodol.*, vol. 115, pp. 41–71, Sep. 2018.

[17] X. Luan, Y. Wang, B. De Schutter, L. Meng, G. Lodewijks, and F. Corman, "Integration of real-time traffic management and train control for rail networks—Part 2: Extensions towards energy-efficient train operations," *Transp. Res. B, Methodol.*, vol. 115, pp. 72–94, Sep. 2018.

[18] S. Su, X. Wang, Y. Cao, and J. Yin, "An energy-efficient train operation approach by integrating the metro timetabling and eco-driving," *IEEE Trans. Intell. Transp. Syst.*, vol. 21, no. 10, pp. 4252–4268, Oct. 2020.

[19] M. Chen, Q. Wang, P. Sun, and X. Feng, "Train control and schedule integrated optimization with reversible substations," *IEEE Trans. Veh. Technol.*, vol. 72, no. 2, pp. 1586–1600, Feb. 2023.

[20] Z. Hou, H. Dong, S. Gao, G. Nicholson, L. Chen, and C. Roberts, "Energy-saving metro train timetable rescheduling model considering ATO profiles and dynamic passenger flow," *IEEE Trans. Intell. Transp. Syst.*, vol. 20, no. 7, pp. 2774–2785, Jul. 2019.

[21] S. Li, R. Liu, Z. Gao, and L. Yang, "Integrated train dwell time regulation and train speed profile generation for automatic train operations on high-density metro lines: A distributed optimal control method," *Transp. Res. B, Methodol.*, vol. 148, pp. 82–105, Jun. 2021.

[22] T. Albrecht, A. Binder, and C. Gassel, "Applications of real-time speed control in rail-bound public transportation systems," *IET Intell. Transp. Syst.*, vol. 7, no. 3, pp. 305–314, Sep. 2013.

[23] P. Wang and R. M. P. Goverde, "Multiple-phase train trajectory optimization with signalling and operational constraints," *Transp. Res. C, Emerg. Technol.*, vol. 69, pp. 255–275, Aug. 2016.

[24] P. Wang, A. Trivella, R. M. P. Goverde, and F. Corman, "Train trajectory optimization for improved on-time arrival under parametric uncertainty," *Transp. Res. C, Emerg. Technol.*, vol. 119, Oct. 2020, Art. no. 102680.

[25] P. Wang and R. M. P. Goverde, "Multi-train trajectory optimization for energy efficiency and delay recovery on single-track railway lines," *Transp. Res. B, Methodol.*, vol. 105, pp. 340–361, Nov. 2017.

[26] P. Wang and R. M. P. Goverde, "Multi-train trajectory optimization for energy-efficient timetabling," *Eur. J. Oper. Res.*, vol. 272, no. 2, pp. 621–635, Jan. 2019.

[27] A. R. Albrecht, P. G. Howlett, P. J. Pudney, X. Vu, and P. Zhou, "Energy-efficient train control: The two-train separation problem on level track," *J. Rail Transp. Planning Manage.*, vol. 5, no. 3, pp. 163–182, Nov. 2015.

[28] J. T. Haahr, D. Pisinger, and M. Sabbaghian, "A dynamic programming approach for optimizing train speed profiles with speed restrictions and passage points," *Transp. Res. B, Methodol.*, vol. 99, pp. 167–182, May 2017.

[29] P. Howlett, P. Pudney, and A. Albrecht, "Optimal driving strategies for a fleet of trains on level track with prescribed intermediate signal times and safe separation," *Transp. Sci.*, vol. 57, no. 2, pp. 399–423, Mar. 2023.

[30] Z. Wang, E. Quaglietta, M. G. P. Bartholomeus, A. Cunillera, and R. M. P. Goverde, "Optimising timing points for effective automatic train operation," *Comput. Ind. Eng.*, vol. 206, Aug. 2025, Art. no. 111237.

[31] J. Pachl, "Timetable design principles," in *Railway Timetabling & Operations*, I. A. Hansen and J. Pachl, Eds., Hamburg, Germany: Eurailpress, 2014, pp. 13–46.

[32] P. Winter, "Potential for benefits with ERTMS," in *Compendium on ERTMS: European Rail Traffic Management System*, P. Winter, Ed., Hamburg, Germany: Eurailpress, 2009, pp. 199–232.

[33] G. M. Scheepmaker, H. Y. Willeboordse, J. H. Hoogenraad, R. S. Luijt, and R. M. P. Goverde, "Comparing train driving strategies on multiple key performance indicators," *J. Rail Transp. Planning Manage.*, vol. 13, May 2020, Art. no. 100163.

[34] A. Albrecht, P. Howlett, P. Pudney, X. Vu, and P. Zhou, "The key principles of optimal train control—Part 2: Existence of an optimal strategy, the local energy minimization principle, uniqueness, computational techniques," *Transp. Res. B, Methodol.*, vol. 94, pp. 509–538, Dec. 2016.

[35] R. M. P. Goverde, G. M. Scheepmaker, and P. Wang, "Pseudospectral optimal train control," *Eur. J. Oper. Res.*, vol. 292, no. 1, pp. 353–375, Jul. 2021.

[36] A. Albrecht, P. Howlett, P. Pudney, X. Vu, and P. Zhou, "The key principles of optimal train control—Part 1: Formulation of the model, strategies of optimal type, evolutionary lines, location of optimal switching points," *Transp. Res. B, Methodol.*, vol. 94, pp. 482–508, Dec. 2016.

Ziyulong Wang received the B.Sc. degree in traffic and transportation from Beijing Jiaotong University in 2018 and the M.Sc. degree in civil engineering from TU Delft in 2020. He currently pursuing the Ph.D. degree with TU Delft. His research focuses on improving the performance of automatic train operation on mainline railway networks in close collaboration with the Dutch Railway Infrastructure Manager ProRail. He has contributed to various railway research and industrial projects, including Europe's Rail MOTIONAL and RAILS. His research interests include public transport, automatic train operation, railway traffic management, data analytics and applied network science. He is currently an Associate Member with the Institution of Railway Signal Engineers (IRSE) and a Member of the International Association of Railway Operations Research (IAROR).

Egidio Quaglietta received the Ph.D. degree in simulation-based signalling optimisation. He is currently an Assistant Professor of railway traffic management with TU Delft. He has been intensively working in the field of railway signalling, since 2008. He has worked as a Research and Development Engineer in several prominent railway companies, such as Italian railway system supplier Ansaldo STS and a British Railway Infrastructure Manager Network Rail, where he led a workstream of the R&I Program "Digital Railway" as well as the sub-project on "Operations for Enhanced Capacity" for the EC FP7 Project Capacity for Rail (C4R). He has developed the simulation tool EGTRAIN. His main interests include railway traffic and infrastructure optimisation, innovative signalling technology, and automated railway operations. He is a Member of the Institution of Railway Signal Engineers (IRSE).

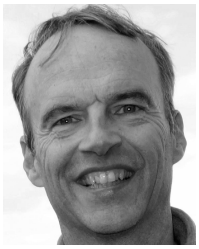

Maarten Bartholomeus received the M.Sc. degree in Physics. Since 2007, has been working as an ERTMS Expert with the Dutch Infrastructure Manager ProRail. With more than twenty-five years of experience in ERTMS, he has been involved in several railway projects as an Engineer, Consultant, Project Manager, and Assessor. In his role as an ERTMS expert, he is responsible for the Dutch ERTMS engineering rules, project specifications, and user processes. He actively cooperates with the ERTMS User Group and European Railway Agency in establishing specifications, and guidelines for ERTMS. Additionally, he participates in multiple european workgroups, focusing on specification improvements and innovations, such as ATO. He also holds a train driver's license and is one of the founders of the Hybrid Level three concept, as well as a co-author of the Hybrid Train Detection principles.

Rob M. P. Goverde (Member, IEEE) received the M.Sc. degree in mathematics from Utrecht University, The Netherlands, in 1993, the Engineering Doctorate (EngD) degree in mathematical modeling and decision support, and the Ph.D. degree in railway transport from TU Delft, in 1996 and 2005, respectively. He is currently a Professor of railway traffic management and operations and the Director of the Digital Rail Traffic Laboratory, TU Delft. He has cooperated in many international research projects, including the EU Projects ON-TIME, MOVINGRAIL, RAILS, PERFORMINGRAIL, SORTEDMOBILITY, and MOTIONAL. He co-authored over 80 journal articles. His research interests include railway timetabling and traffic management, automatic train operation, train control, and railway signalling. He is Fellow of the Institution of Railway Signal Engineers (IRSE). He served as an Associate Editor for IEEE TRANSACTIONS ON INTELLIGENT TRANSPORTATION SYSTEMS and is the Editor-in-Chief of *Journal of Rail Transport Planning and Management*. He is the President of the International Association of Railway Operations Research (IAROR).